

Synthesis of Gold Nanorod/Single-Wall Carbon Nanotube Heterojunctions Directly on Surfaces

Aneta J. Mieszawska,[†] Romaneh Jalilian,[‡] Gamini U. Sumanasekera,[‡] and Francis P. Zamborini^{*†}

Departments of Chemistry and Physics, University of Louisville, Louisville, Kentucky 40292

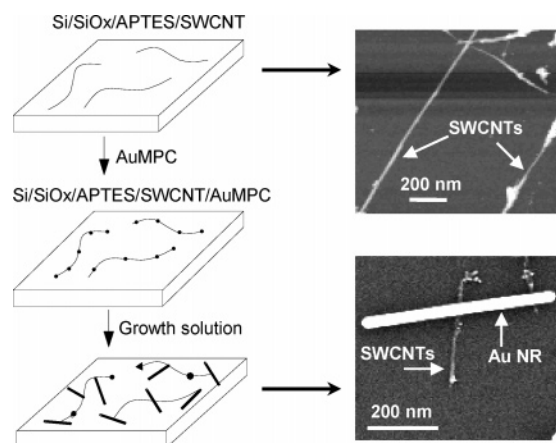
Received April 2, 2005; E-mail: f.zamborini@louisville.edu

In this communication we describe the formation of heterojunctions between metallic one-dimensional (1D) gold nanorods (Au NRs) and single-wall carbon nanotubes (SWCNTs) assembled directly on surfaces. The synthesis of multicomponent structures with junctions of different 1D materials is important for many electronic,¹ optoelectronic,² and sensing applications.³ Carbon-semiconductor (SC),^{1a} SC-metal,^{1b,c} carbon-metal,^{1c,d} carbon-carbide,^{1e} and SC-SC² 1D heterojunctions have been fabricated and shown to exhibit Schottky diode behavior,^{1a} Ohmic contact,^{1d,e} thermoelectric properties,^{2a} photoluminescence,^{2c} and electroluminescence.^{2c} Striped nanorods composed of different metal-metal junctions have served as biobarcode sensors.³ Previous methods have led mostly to end-to-end junctions by electrochemical deposition in porous templates,^{1b-d,3} a solid-solid reaction,^{1e} or vapor-phase growth onto catalysts.^{1a,2}

Heterojunctions of 1D semi-crystalline metals and SWCNTs as described in this paper have not been previously fabricated. Other metal-carbon junctions involving Au nanoparticles and SWCNTs⁴ or 1D amorphous carbon and 1D polycrystalline metal^{1c,d} have appeared. Our work represents a new type of structure with many benefits. First, the procedure is quick and simple and can be performed with commercially available reagents on a benchtop without the need for high-temperature reactors, templates, or potentiostats. Second, the heterojunctions form by growing Au NRs on the SWCNTs with high selectivity and without altering the electronic structure of the CNTs. Third, they are formed directly on surfaces; therefore, it is not necessary to suspend, separate, and deposit the structures on a surface after synthesis. Patterning and alignment should be possible with current strategies used for CNTs. Fourth, there are several potential applications for these structures. For example, Au NRs may serve as tiny, reproducible electrical contacts for integrating SWCNTs in nanoelectronic or sensing devices, metal nanostructures of various shapes supported on SWCNTs may be useful in electrocatalysis or electrochemical sensing applications, and as demonstrated in this paper, the Au nanostructures enhance Raman scattering of SWCNTs.

Au NR/SWCNT heterojunctions were synthesized directly on Si/SiO_x substrates by the three steps shown in Scheme 1 (see Supporting Information for full details). First, SWCNTs were deposited onto (aminopropyl)triethoxysilane (APTES)-functionalized Si/SiO_x by soaking the substrate in a dilute dimethylformamide solution of SWCNTs for 20–25 min. The top atomic force microscopy (AFM) image in Scheme 1 shows a few SWCNT bundles (typically 5–10 nm in diameter containing 25–100 NTs) adsorbed to Si/SiO_x/APTES through surface NH₂ groups. Second, the substrate is placed into a 9 mg/mL solution of 1.6 nm average diameter hexanethiolate Au monolayer-protected clusters (MPCs)⁵ for 10–15 min. The MPCs adsorb to SWCNTs presumably through hydrophobic interactions, which should not alter the electronic

Scheme 1



properties of the SWCNTs. Finally, the substrate was placed into a “growth solution” for 1 h containing HAuCl₄, cetyltrimethylammonium bromide (CTAB), and ascorbic acid. This leads to the seed-mediated growth of the SWCNT-bound Au MPCs into Au NRs and other shapes as described previously.⁶ The bottom SEM image in Scheme 1 shows a crossed Au NR/SWCNT junction formed using this procedure.

Figure 1 shows various SEM images of different regions of a surface containing Au NR/SWCNT heterojunctions. Close inspection of several images shows that >90% of the Au nanostructures emanate directly from SWCNTs, consistent with the model in Scheme 1. There are usually only one to two Au nanostructures per SWCNT due to the weak hydrophobic interactions involved. The yield of NRs versus other shapes is ~19%, which is slightly higher than high aspect ratio (AR) Au NRs grown in solution^{6a} and on surfaces^{6b-d} by seed-mediated growth. The diameter of NRs is fairly uniform (25–30 nm), and the average length is 572 ± 203 nm (AR ≈ 20). The seed-mediated growth process is not fully understood, but it is believed that anisotropic growth into Au NRs is promoted by preferential adsorption of CTAB onto certain crystal faces of Au.

Different types of junctions form between the NRs and SWCNTs. Scheme 1 showed an example where the Au MPC grew from the CNT in two directions^{6d} to form a crossed NR/NT junction. NT 1 and NR 1 in Frame A of Figure 1 represents a NR growing from a NT in one direction, where it is connected to the CNT, but not crossing it. The NR 2/NT 2 junction is another example of a cross junction, but the NR is at the end of the bundle of NTs. Different types of extended junctions are also common. Frame B shows an example of one Au NR connecting three NT bundles (NT 3, NT 4, and NT 5). Frame C shows an example of two Au NRs (NR 3 and NR 4) connected to the same bundle of NTs (NT 6 and NT 7). It is difficult to see, but NT 7 extends all the way to NR 4. The NRs in this configuration could serve as contacts to the NTs for electronic

[†] Department of Chemistry.

[‡] Department of Physics.

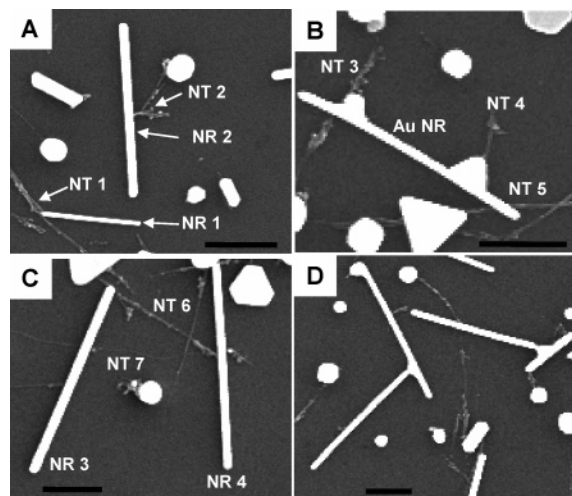


Figure 1. SEM images of Au NR/SWCNT heterojunctions. (A) NRs attached to the side wall and end of nanotubes from Au MPCs grown in one (NR 1) or two (NR 2) directions. (B) Au NR attached to three different SWCNT bundles (NT 3, NT 4, and NT 5). (C) Two Au NRs (NR 3 and NR 4) attached to the same bundle of SWCNTs (NT 6 and NT 7). (D) Connection between six NRs and at least eight different SWCNT bundles. Scale bars are 250 nm.

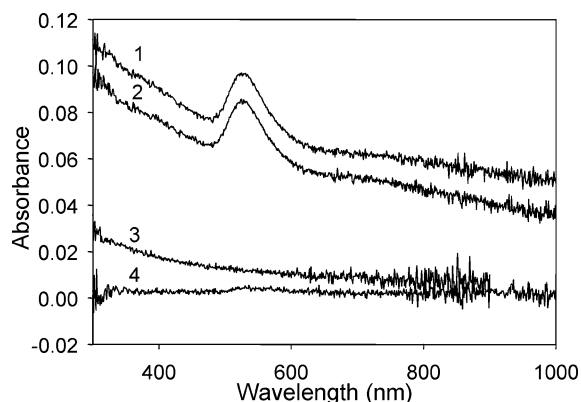


Figure 2. Visible spectra of (1) glass/APTES/SWCNT/Au MPCs (15 min), (2) glass/APTES/SWCNT/Au MPCs (10 min), (3) glass/APTES/SWCNTs (2 days), and (4) glass/APTES/Au MPCs (15 min) placed in growth solution for 1 h.

and chemiresistive sensing applications. Frame D shows an example of several NRs and NTs interconnected. Since it is difficult to resolve very tiny bundles or individual SWCNTs with SEM, some of the NTs appear disconnected, but are actually continuous. We are currently studying the electronic properties of various junctions by depositing metal contacts via electron-beam lithography.

Figure 2 demonstrates conclusively that Au grows selectively on the SWCNTs. Plots 1 and 2 are the visible spectra of glass/APTES/SWCNT samples that were placed in Au MPCs for 15 and 10 min, respectively, and then into growth solution for 1 h to form Au NR/SWCNT heterojunctions. The large absorbance in the visible region and the surface plasmon (SP) band at 527 nm are consistent with the formation of Au nanostructures on the surface. The substrate soaked for 15 min has a higher absorbance compared to that for 10 min due to the larger coverage of Au MPCs. Plots 3 and 4 are the visible spectra of glass/APTES/SWCNTs (no Au MPCs) placed in growth solution for 1 h and glass/APTES placed in Au MPCs for 15 min and then into growth solution for 1 h, respectively. Neither sample exhibits significant absorbance or evidence of a SP band for Au, indicating that Au MPCs do not adsorb appreciably to the glass/APTES surface and that neither glass/APTES nor SWCNTs (without MPCs) catalyze the growth

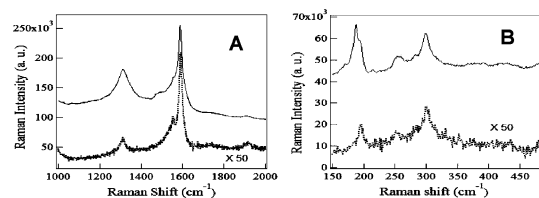


Figure 3. Raman spectra depicting (A) G and D bands in the high-frequency regime and (B) radial breathing mode in the low-frequency regime of SWCNTs for pristine (bottom spectra) and Au NR-SWCNT heterojunctions (top spectra). The spectra were collected at 632.8 nm excitation using a Renishaw micro Raman system.

of Au nanostructures. This key experiment confirms that Au NRs grow directly from the Au MPCs bound to SWCNTs as depicted in Scheme 1.

Raman spectroscopy is commonly used to characterize SWCNTs,^{7a,b} and Au NRs are known to enhance Raman scattering signals.^{7c} Figure 3A,B shows the high-frequency regime (containing G and D bands) and low-frequency regime (containing radial breathing modes), respectively, of the spectrum of SWCNTs before (bottom spectrum) and after growth of Au NRs and other nanostructures (top spectrum).^{7a,b} The presence of Au enhanced the SERS signal 50-fold. We believe that intimate contact made between the Au and SWCNTs resulting from our procedure is important for enhancement.

We have described a simple chemical method for synthesizing surface-attached 1D Au NR/SWCNT heterojunctions. These new structures are interesting fundamentally and have promising applications. Better synthetic control, patterning, and alignment of junctions are still needed. Research on these issues and the electronic and Raman enhancement properties are underway.

Acknowledgment. This research was partially funded through the University of Louisville by an intramural Research Incentive Grant from the Office of the Senior Vice President of Research.

Supporting Information Available: More detailed description of synthesis. This material is available free of charge via the Internet at <http://pubs.acs.org>.

References

- (1) (a) Hu, J.; Ouyang, M.; Yang, P.; Lieber, C. M. *Nature* **1999**, *399*, 48–51. (b) Kovtyukhova, N. I.; Kelley, B. K.; Mallouk, T. E. *J. Am. Chem. Soc.* **2004**, *126*, 12738–12739. (c) Luo, J.; Zhang, L.; Zhang, Y.; Zhu, J. *Adv. Mater.* **2002**, *14*, 1413–1414. (d) Luo, J.; Huang, Z.; Zhao, Y.; Zhang, L.; Zhu, J. *Adv. Mater.* **2004**, *16*, 1512–1515. (e) Zhang, Y.; Ichihashi, T.; Landree, E.; Nihey, F.; Iijima, S. *Science* **1999**, *285*, 1719–1722.
- (2) (a) Bjork, M. T.; Ohlsson, B. J.; Sass, T.; Persson, A. I.; Thelander, C.; Magnusson, M. H.; Deppert, K.; Wallenberg, L. R.; Samuelson, L. (b) Wu, Y.; Fan, R.; Yang, P. *Nano Lett.* **2002**, *2*, 83–86. (c) Gudiksen, M. S.; Lathon, L. J.; Wang, J.; Smith, D. C.; Lieber, C. M. *Nature* **2002**, *415*, 617–620.
- (3) Nicewarner-Peña, S. R.; Freeman, R. G.; Reiss, B. D.; He, L.; Peña, D. J.; Walton, I. D.; Cromer, R.; Keating, C. D.; Natan, M. J. *Science* **2001**, *294*, 137–141.
- (4) (a) Choi, H. C.; Shim, M.; Bangsaruntip, S.; Dai, H. *J. Am. Chem. Soc.* **2002**, *124*, 9058–9059. (b) Ellis, A. V.; Vijayamohan, K.; Goswami, R.; Chakrapani, N.; Ramanathan, L. S.; Ajayan, P. M.; Ramanath, G. *Nano Lett.* **2003**, *3*, 279–282.
- (5) Brust, M.; Fink, J.; Schiffrin, D. J.; Kiely, C. *J. Chem. Soc., Chem. Commun.* **1995**, 1655–1656.
- (6) (a) Jana, N. R.; Gearheart, L.; Murphy, C. J. *J. Phys. Chem. B* **2001**, *105*, 4065–4067. (b) Taub, N.; Krichevski, O.; Markovich, G. *J. Phys. Chem. B* **2003**, *107*, 11579–11582. (c) Wei, Z.; Mieszawska, A. J.; Zamborini, F. P. *Langmuir* **2004**, *20*, 4322–4326. (d) Wei, Z.; Zamborini, F. P. *Langmuir* **2004**, *20*, 11301–11304.
- (7) (a) Rao, A. M.; Richter, E.; Bandow, S.; Chase, B.; Eklund, P. C.; Williams, K. A.; Fang, S.; Subbaswamy, K. R.; Menon, M.; Thess, A.; Smalley, R. E.; Dresselhaus, G.; Dresselhaus, M. S. *Science* **1997**, *275*, 187–191. (b) Kneipp, K.; Perelman, L. T.; Kneipp, H.; Backman, V.; Jorio, A.; Dresselhaus, G.; Dresselhaus, M. S. *Phys. Rev. B* **2001**, *63*, 193411. (c) Nikoobakht, B.; Wang, J.; El-Sayed, M. A. *Chem. Phys. Lett.* **2002**, *366*, 17–23.

JA0521122